IFSCC 2025 full paper (N° IFSCC2025-1277)

"Scalable production and characterization of silk-based emulsion for cosmetic application"

Firdaws Mahboubi[1, 2], Laurianne SIMON[1], Thomas-Xavier METRO[1], Christophe DO-RANDEU[1], Sylvie BEGU [1,*]

[1]ICGM, Univ Montpellier, CNRS, ENSCM, Montpellier, France ; [2] Benu Blanc,1 chemin du Tracollet 38113 Veurey-Voroize, Grenoble,

1. Introduction

Silk has been renowed for thousands of years in the textile industry as a luxury material thanks to its luster and mechanical properties. The most commonly used silk is Bombyx mori silk, also known as mulberry silk. Mulberry silk is composed of two proteins: fibroin fibers core coated with glue-like protein called sericin [1]. The silk proteins have been widely used in various applications ranging from food, health and cosmetics. In the realm of cosmetics, silk proteins are gaining increasing attention thanks to their numerous effects on the skin: moisturization [2], anti-aging properties [3], wound healing [4]. In addition to that, many researchers have studied the emulsifying capacity of silk – mostly fibroin – as a stabilizer in various types of emulsion formulations: gel-emulsions [5,6], film-stabilized emulsions [7,8] and Pickering emulsions [9–13]. Nevertheless, most of these formulations rely on multi-step bottom-up methods that involve solvents, which limit scalability and, consequently, industrial applications. Consequently, this study proposes an alternative top-down approach (Cosmos approved) via milling to obtain silk particles and explores the influence of milling parameters on the emulsifying properties of the particles. These silk particles (COSMOS Bio-labelled) will later serve as Pickering emulsion stabilizers without the need for solvents or surfactants.

2. Materials and Methods

Materials

Silk cocoons were purchased from China. Paraffin oil from Sigma-Aldrich (Germany). Olive oil and Caprylic/Capric Triglyceride were obtained from local supermarkets in Montpellier (France).

Methods

2.1 Degumming process:

Silk cocoons were first cut into 1cm pieces, then degummed using autoclave VMR Vapour-Line (VMR international,India) at 121°C for 20 min with a cocoon distilled water ratio of 1:25 (w/v). Then, fibroin fibers were washed thoroughly with tap water and rinsed by distilled water, then dried at 45°C for 12 hours.

2.2 Milling process

The milling process consisted on 3 steps. First, fibroin fibers were pre-milled using a crusher equipped with 4 blades (Pulverisette 29 from Fritsch GmbH, Germany) at a speed of 2900 rpm until they passed through a sieve of 1 mm. Second, the obtained pre-milled fibers were dry milled using planetary ball mill (Pulverisette 7 Premium Line from Fritsch GmbH, Germany) equipped with 20 ml zirconium oxide grinding jar and 10 zirconium oxide balls of 10 mm . The process was optimized with 12 cylces of 2 minutes milling with 8 minutes pause between milling cycles to obtain dry milled particles (DMP). Third, the DMP were wet milled using 30g of 0.5 mm zirconium oxide balls and adding 4 ml of distilled water. The same milling process of cycles of 2 minutes and 8 minutes pause was applied to obtain a suspension of wet milled particles (WMP).

2.3 Particle size analysis

The resulting fibroin particles (DMP and WMP) were characterized in terms of size distribution with laser diffraction 3000 Master sizer (Malvern Instruments, UK) using refractive index of silk of 1.561. Prior to measurements, DMP were dispersed in distilled water and sonicated with sonicator probe S-250 (Branson Ultrasonics, USA) at duty cycle:40%, output: 2 and timer: 2 minutes.

Then, powder suspension were filtrated on 0.650 µm filter (Sartorius stedim EO filter) and analyzed with Dynamic light scattering Zetasizer NanoZS apparatus (Malvern Instruments, UK) equipped with a He-Ne laser (632.8 nm). The hydrodynamic diameter and polydispersity index (PDI) of present nanoparticles were evaluated at a dilution factor of 400. The measurements were conducted at 20 °C with a scattering angle of 173°.

2.4 Scanning electron microscopy

Silk fibers and silk particles were observed under scanning electron microscopy with SEM S-2600N (HITACHI, Japan). The particles were covered with platinum prior to observation.

2.5 Contact angle

Silk particles wettability was assessed using contact angle measurements by sessile drop methods on silk particles tablets. 80 mg of silk fibroin powder were compressed using

SPECAC® with a 6 tons force for 1min to form a tablet. Contact angle measurements were performed using the sessile drop method with OCA optical contact angle goniometer (Dataphysics Instruments, Germany). A droplet of water (~3 µL) was gently placed on the surface of the pellet, and the contact angle was measured immediately using image analysis software (SCA20-U software). All measurements were conducted at 25°C.

2.6 Surface tension measurements

The reduction of surface tension at air/water interface was followed using the Wilhelmy plate method on K100 Krüss Processor Tensiometer (Krüss GmbH, Germany), . A concentration range of dry milled particles (DMP) and wet milled particles (WMP) from 0.1 to 0.75 % w/v was prepared in MilliQ water. Prior to measurements, the suspensions of DMP were sonicated using a sonication probe S-250 (Branson Ultrasonics, USA) at duty cycle: 40 %, output: 2 and timer: 2 minutes. DMP and WMP suspensions were left to equilibrate for 5 minutes before measurements. Data were collected at 25 °C, a detection speed of 6 mm/min, detection sensitivity of 0.01 g and immersion depth of 2 mm using the Krüss software. A blank measurement was first performed using ultrapure water (γ=69–73 mN).

2.7 Fourier-transform infrared spectroscopy

Fourier Transform Infrared (FTIR) spectroscopy was performed using an ATR-FTIR spectrometer (PerkinElmer®, USA). Spectra were collected in the range of 400–4000 cm^{-1}, with 4 scans accumulated per sample. Wet milled particles (WMP) was lyophilized prior to analysis.

2.8 Emulsification tests:

Oil-in-water Pickering emulsions were obtained by mixing dry milled particles DMP or wet milled particles WMP suspensions in distilled water and paraffin oil in different ratios. The mixture was put in an ice bath as a cooling system, and then was subjected to sonication using a sonication probe S-250 (Branson Ultrasonics, USA) with an output of 2, duty cycle of 40 % and timer 2 minutes.

3. Results

3.1 Degumming process:

Observation of surface morphology of silk fibers on scanning electron microscopy before and after the degumming process shows raw silk fibers exhibiting a rough and irregular surface, with a dense coating layer covering the fibroin core. This outer layer is attributed to the

presence of sericin (Figure.1 (a)). After degumming, the fibers appeared smoother and more defined, with the sericin layer effectively removed (Figure.1 (b)).

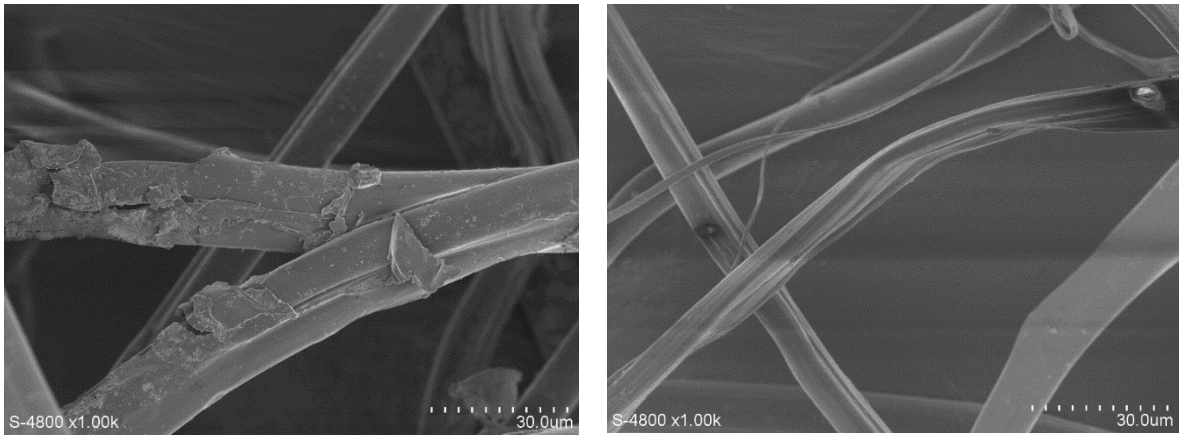

(**a**) (**b**)

Figure 1. SEM images of raw silk fibers before degumming (a) and after degumming (b). Scale bar = 30.0 µm. Magnification = x1000.

3.2 Particle size analysis:

Particle size distributions of silk particles were evaluated using both laser diffraction and dynamic light scattering (DLS). The volume-based size distribution for DMP (dry milled particles) and WMP (wet milled particles) is presented in Figure 2 (a). Laser diffraction analysis of DMP showed a main peak centered at approximately 94 µm. For WMP, 2 peaks are observed, centered at 3 µm and near 800 nm. DLS measurements of WMP 0.65 µm filtered suspension, indicated a Z-average diameter of 464.4 nm with a polydispersity index (PDI) of 0.24. The intensity-based distribution obtained from DLS is shown in Figure Figure 2. (b).

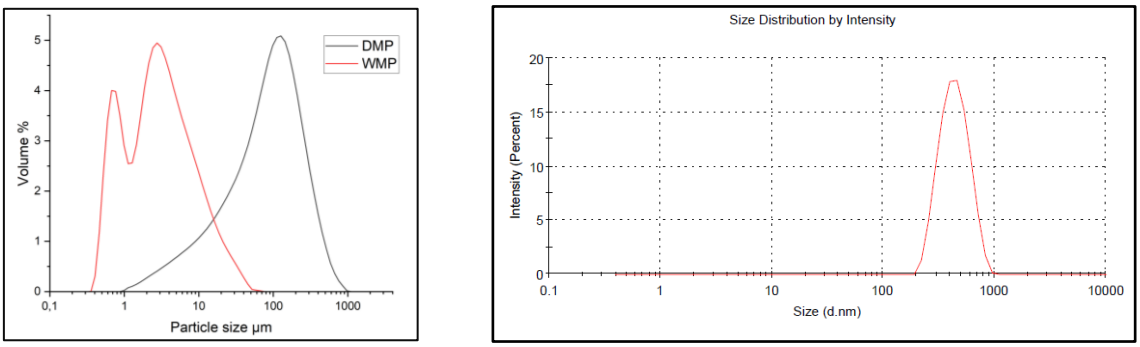

(**a**) (**b**)

Figure 2. (a) Particle size (µm) of DMP and WMP (b) Dynamic light scaterring particle size distribution by intensity of 0.65µm filtered WMP suspension.

SEM was used to visualize the particles morphology (Figure 3). SEM images demonstrated the roughness and irregular shape of DMP (Figure 3.a) compared to spherical morphology of aggreagted WMP (Figure 3.b).

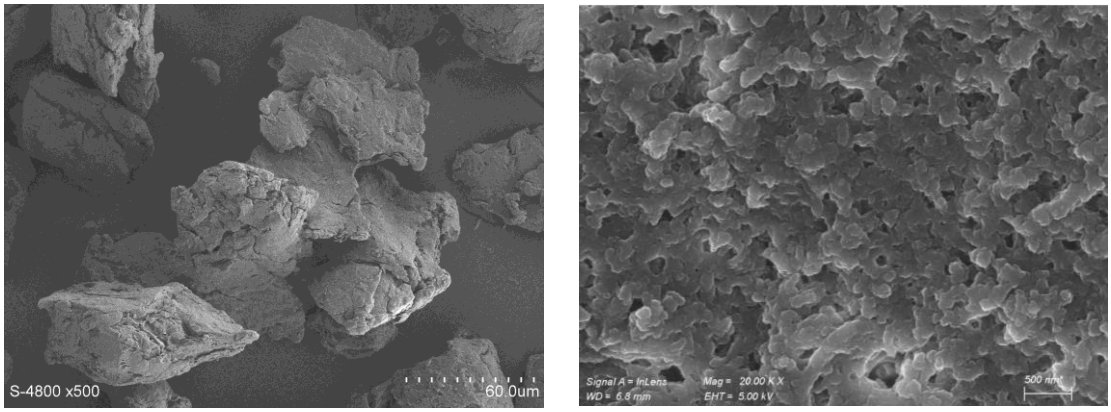

(**a**) (**b**)

Figure 3. Scanning electron microscopy images of (a) DMP (Scale bar= 60.0 µm. Magnification = x500). (b) lyophilized WMP (Scale bar= 500nm. Magnification = x20,000x)

3.3 Contact angle and surface tension measurements:

The wettability of silk particles was assessed by contact angle measurements. For both DMP and WMP the contact angle was similar close to 52° (Table 1).

Table 1. Contact angle at air/water of milled particles DMP and WMP

Particle type	DMP	WMP
Contact angle θ (water/air)	52.36°	52.8°

To investigate the effect of particle type and concentration on the interfacial properties, air-water surface tension measurements were conducted at ambient temperature (Figure 4.(a)). The addition of DMP (dry milled particles) led to a marked decrease in surface tension, dropping from 72.8 mN/m to 50 mN/m at a concentration of 0.1% (w/v), beyond which the values reached a plateau, indicating saturation at the interface. In contrast, WMP (wet milled particles) exhibited lower reduction, lowering the surface tension to 66.94 mN/m at the same concentration. Upon further increase in concentration, WMP reached a plateau around 60 mN/m, suggesting a lower interfacial activity compared to DMP.

3.4 Fourier-transform infrared spectroscopy

Fourier-transform infrared (FTIR) spectroscopy was employed to assess the chemical composition of DMP (dry milled particles) and WMP (wet milled particles) particle surface. As shown

in Figure 4. (b), all samples display highly similar spectra, with similar peak positions: 3276cm^{-1}, 1622cm^{-1} and 1518cm^{-1} for WMP compared to 3277cm^{-1}, 1632cm^{-1} and 1516cm^{-1} for DMP.

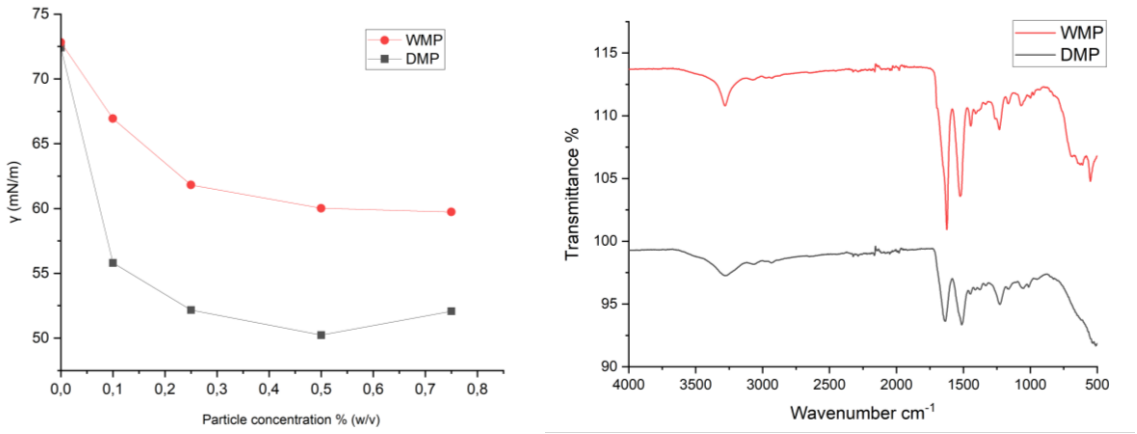

(**a**) (**b**)

Figure 4. (a) Effect of particle type/ particle concentration on surface tension at the air/water interface (b) FTIR spectra of DMP and WMP

3.5 Emulsification tests:

Results of emulsion tests with paraffin oil using both DMP (dry milled particles) and WMP (wet milled particles) are presented in Figure 5.

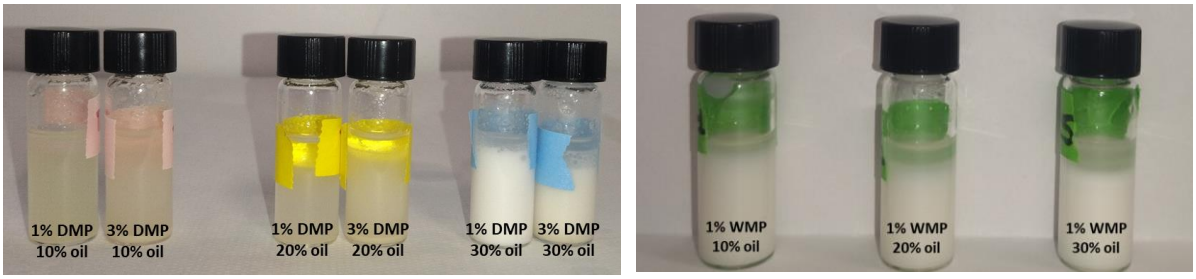

(**a**) (**b**)

Figure 5. Results of emulsification tests on (a) DMP ; (b) WMP with paraffin oil at different ratios

Increasing the oil concentration enabled emulsion formation with DMP; however, a small fraction of oil consistently remained at the surface. In contrast, increasing the oil concentration in the presence of WMP did not lead to emulsion formation. As shown in Figure 5(b), the white appearance corresponds to nanoparticle suspension, with the oil phase clearly visible at the surface.

Based on these observations, a stable formulation containing 30% (w/w) oil and 1% (w/w) DMP was selected to further evaluate the emulsifying capacity of DMP with olive oil (Figure

6(a)) and caprylic/capric triglyceride (Figure 6(b)). In both cases, a minor oil fraction remained at the surface, consistent with the behavior observed with paraffin oil.

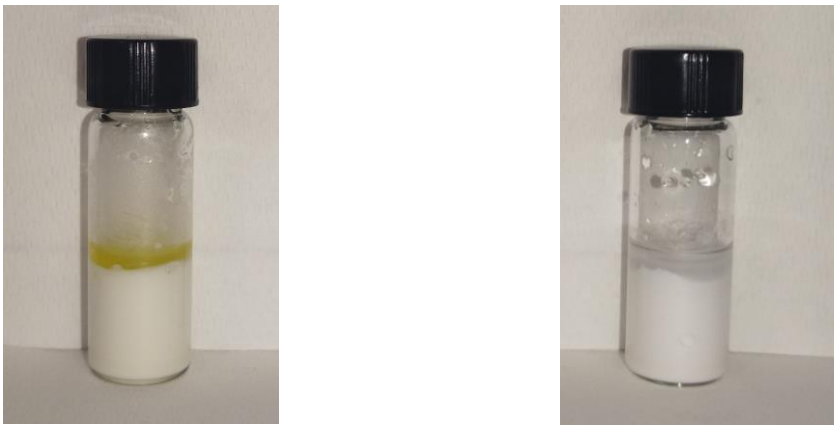

(**a**) (**b**)

Figure 6. Results of emulsion tests with 1% DMP and 30% (a) olive oil (b) caprylic/capric triglyceride.

Microscopic observation at 10x magnification of 30% paraffin oil (Figure 7(a)) and 30% olive oil (Figure 7(b)) showcases a fine droplet distribution, resembling a carpet, surrounded by particles.

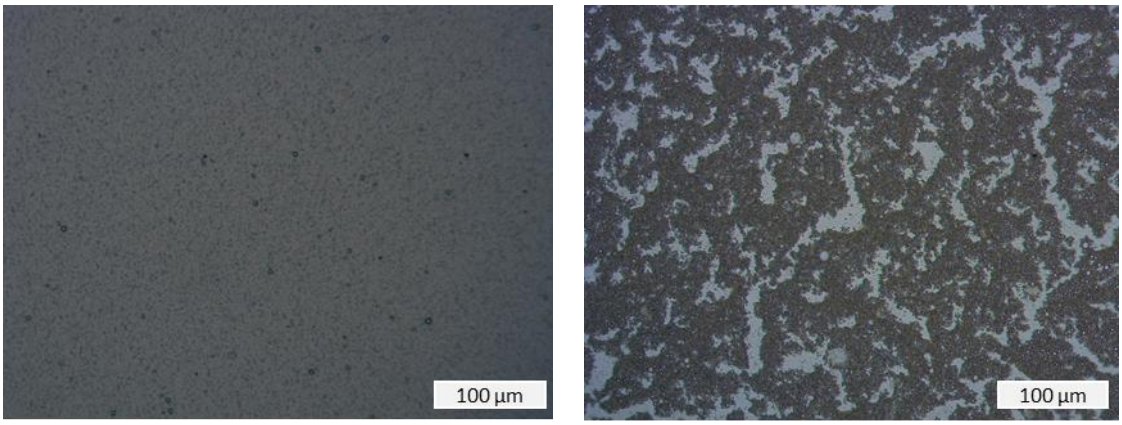

(**a**) (**b**)

Figure 7. Microscopic observation of emulsion of paraffin oil (a) and olive oil (b) at the same concentration of oil (30% w/w) and DMP (1% w/w). Magnification x10.

4. Discussion

The formulation of Pickering emulsions relies on several particle properties, including particle wettability characterized by the contact angle Θ, particle size , roughness, shape and concentration [14]. These parameters are also influenced by milling process parameters. In this study,

we investigated the emulsifying properties of silk fibroin particles obtained through dry and wet milling processes. As expected, the milling process induced different size distribution of silk fibroin particles (Figure 2). The second milling step resulted in microparticles (DMP) with a median diameter (D_{50}) of 94 µm measured by laser diffraction. An additional third step with distilled water yielded nanoparticles, with a volume peak at 800 nm and a smaller peak around 400 nm observed by dynamic light scattering (DLS). Scanning electron microscopy confirmed the presence of nanoparticle aggregates, with individual particle sizes around 50 nm. Compared to previous studies on silk milling, we optimized a three-step milling process and we achieved nanoscale particles more rapidly. None of the previous studies addressed the influence of milling parameters on the emulsifying properties of the resulting particles. However, the shape and surface characteristics of these nanoparticles differed across studies, in function of milling process and equipment. Notably, nanoparticle aggregation was consistently observed in all cases, including our own [15–17]. Given the significant size difference, we compared the emulsifying performance of microparticles and nanoparticles derived from the same silk fibroin source. Both particle types exhibited similar contact angles (~52°), suggesting a moderately hydrophilic surface. However, it is important to interpret these contact angle measurements cautiously, as compressing the powders into pellets for analysis likely alters critical surface properties, such as porosity, that can strongly influence wettability. Infrared spectroscopy revealed similar absorption peaks for both particle types, indicating comparable surface chemistry. However, differences emerged when evaluating interfacial activity. Microparticles were able to significantly reduce surface tension, whereas the nanoparticles showed little effect. This finding was consistent with emulsification experiments: under identical conditions of oil and particle concentration, only the microparticles (DMP) successfully stabilized an emulsion, while the nanoparticles/ aggregated nanoparticles (WMP) failed to do so.These results highlight the significant influence of milling parameters not only on particle size, but potentially on other characteristics—such as surface structure and porosity—that impact emulsifying capacity. While particle size is a major factor, the inability of nanoparticles to reduce surface tension suggests that other physical attributes altered during milling may be equally important. Microscopic examination of emulsions stabilized with DMP revealed a fine droplet distribution about 20µm. Interestingly, large microparticles appeared to stabilize small droplets, a phenomenon not yet fully understood. We hypothesize that the particles may form a dispersed matrix that "traps" oil droplets rather than coating them in a traditional Pickering stabilization mechanism [18]. For future studies, it would be valuable to explore alternative emulsification techniques—such as high-pressure homogenization or Ultra-Turrax mixing—to further evaluate the performance of these particles under different shear conditions. Overall, this study highlights the importance of milling parameters on the emulsifying properties of silk fibroin particles.

These findings are particularly relevant for future industrial applications of milled natural polymers as eco-friendly stabilizers in emulsion-based formulations.

5. Conclusion

This study demonstrates that the emulsifying properties of silk fibroin particles are strongly influenced by milling parameters. Although both microparticles and nanoparticles derived from the same fibroin source exhibited similar surface chemistry and contact angles, only the microparticles effectively stabilized oil-in-water emulsions and reduced surface tension. To build on these findings, future investigations should explore additional factors that may influence emulsification, such as surface structure and porosity, which are likely to play a significant role. The unexpected ability of larger particles to stabilize fine droplets—possibly through a trapping mechanism—offers promising perspectives for the development of bio-based stabilizers. Further research should also investigate the impact of alternative emulsification techniques and delve deeper into the structural characteristics of milled particles to optimize their performance in industrial applications.

References:

(1) Pereira, R. F. P.; Silva, M. M.; De Zea Bermudez, V. *Bombyx Mori* Silk Fibers: An Outstanding Family of Materials: *Bombyx Mori* Silk Fibers: An Outstanding Family …. *Macromol. Mater. Eng.* **2015**, *300* (12), 1171–1198. https://doi.org/10.1002/mame.201400276.

(2) Daithankar, A. V.; Padamwar, M. N.; Pisal, S. S.; Paradkar, A. R.; Mahadik, K. R. Moisturizing Efficiency of Silk Protein Hydrolysate: Silk Fibroin. *Indian J. Biotechnol.* **2005**, *4*, 115–121.

(3) Tsubouchi, K.; Nakao, H.; Igarashi, Y.; Takasu, Y.; Yamada, H. *Bombyx Mori* Fibroin Enhanced the Proliferation of Cultured Human Skin Fibroblasts. The Japanese Society of Sericultural Science 2003. https://doi.org/10.11416/jibs.72.65.

(4) Ju, H. W.; Lee, O. J.; Moon, B. M.; Sheikh, F. A.; Lee, J. M.; Kim, J.-H.; Park, H. J.; Kim, D. W.; Lee, M. C.; Kim, S. H.; Park, C. H.; Lee, H. R. Silk Fibroin Based Hydrogel for Regeneration of Burn Induced Wounds. *Tissue Eng. Regen. Med.* **2014**, *11* (3), 203–210. https://doi.org/10.1007/s13770-014-0010-2.

(5) Pritchard, E. M.; Normand, V.; Hu, X.; Budijono, S.; Benczédi, D.; Omenetto, F.; Kaplan, D. L. Encapsulation of Oil in Silk Fibroin Biomaterials. *J. Appl. Polym. Sci.* **2014**, *131* (6), app.39990. https://doi.org/10.1002/app.39990.

(6) Zhang, H.; Jiang, Q.; Li, J.; Sun, Y.; Zhang, R.; Zhang, L.; Zhang, H. Oil-Droplet Anchors Accelerate the Gelation of Regenerated Silk Fibroin-Based Emulsion Gels. *Int. J. Biol. Macromol.* **2024**, *278*, 134579. https://doi.org/10.1016/j.ijbiomac.2024.134579.

(7) Tang, X.; Qiao, X.; Sun, K. Effect of pH on the Interfacial Viscoelasticity and Stability of the Silk Fibroin at the Oil/Water Interface. *Colloids Surf. Physicochem. Eng. Asp.* **2015**, *486*, 86–95. https://doi.org/10.1016/j.colsurfa.2015.09.030.

(8) Sarquis, I. R.; Sarquis, R. S. F. R.; Marinho, V. H. S.; Neves, F. B.; Araújo, I. F.; Damasceno, L. F.; Ferreira, R. M. A.; Souto, R. N. P.; Carvalho, J. C. T.; Ferreira, I. M. Carapa Guianensis Aubl. (Meliaceae) Oil Associated with Silk Fibroin, as Alternative to Traditional Surfactants, and Active against Larvae of the Vector Aedes Aegypti. *Ind. Crops Prod.* **2020**, *157*, 112931. https://doi.org/10.1016/j.indcrop.2020.112931.

(9) Byrne, N.; DeSilva, R.; Whitby, C. P.; Wang, X. Silk Scaffolds Achieved Using Pickering High Internal Phase Emulsion Templating and Ionic Liquids. *RSC Adv.* **2013**, *3* (46), 24025. https://doi.org/10.1039/c3ra44749a.

(10) Cheng, Q.; Zhang, B.; He, Y.; Lu, Q.; Kaplan, D. L. Silk Nanofibers as Robust and Versatile Emulsifiers. *ACS Appl. Mater. Interfaces* **2017**, *9* (41), 35693–35700. https://doi.org/10.1021/acsami.7b13460.

(11) Hu, Y.; Zou, Y.; Ma, Y.; Yu, J.; Liu, L.; Chen, M.; Ling, S.; Fan, Y. Formulation of Silk Fibroin Nanobrush-Stabilized Biocompatible Pickering Emulsions. *Langmuir* **2022**, *38* (46), 14302–14312. https://doi.org/10.1021/acs.langmuir.2c02376.

(12) Sun, S.; Deng, Y.; Sun, F.; Mao, Z.; Feng, X.; Sui, X.; Liu, F.; Zhou, X.; Wang, B. Engineering Regenerated Nanosilk to Efficiently Stabilize Pickering Emulsions. *Colloids Surf. Physicochem. Eng. Asp.* **2022**, *635*, 128065. https://doi.org/10.1016/j.colsurfa.2021.128065.

(13) Huang, S.; Peng, J.; Zi, Y.; Zheng, Y.; Xu, J.; Gong, H.; Kan, G.; Wang, X.; Zhong, J. Regenerated Silk Fibroin for the Stabilization of Fish Oil-Loaded Pickering Emulsions. *Colloids Surf. Physicochem. Eng. Asp.* **2023**, *678*, 132523. https://doi.org/10.1016/j.colsurfa.2023.132523.

(14) Ming, L.; Wu, H.; Liu, A.; Naeem, A.; Dong, Z.; Fan, Q.; Zhang, G.; Liu, H.; Li, Z. Evolution and Critical Roles of Particle Properties in Pickering Emulsion: A Review. *J. Mol. Liq.* **2023**, *388*, 122775. https://doi.org/10.1016/j.molliq.2023.122775.

(15) Kazemimostaghim, M.; Rajkhowa, R.; Tsuzuki, T.; Wang, X. Production of Submicron Silk Particles by Milling. *Powder Technol.* **2013**, *241*, 230–235. https://doi.org/10.1016/j.powtec.2013.03.004.

(16) Rajkhowa, R.; Wang, L.; Wang, X. Ultra-Fine Silk Powder Preparation through Rotary and Ball Milling. *Powder Technol.* **2008**, *185* (1), 87–95. https://doi.org/10.1016/j.powtec.2008.01.005.

(17) Rajkhowa, R.; Wang, L.; Kanwar, J.; Wang, X. Fabrication of Ultrafine Powder from Eri Silk through Attritor and Jet Milling. *Powder Technol.* **2009**, *191* (1–2), 155–163. https://doi.org/10.1016/j.powtec.2008.10.004.

(18) Li, Z.; Ngai, T. Macroporous Polymer from Core−Shell Particle-Stabilized Pickering Emulsions. *Langmuir* **2010**, *26* (7), 5088–5092. https://doi.org/10.1021/la903546g.